THE JOURNAL OF PHYSICAL CHEMISTRY B

Article

pubs.acs.org/JPCB

A Refined All-Atom Potential for Imidazolium-Based Room Temperature Ionic Liquids: Acetate, Dicyanamide, and Thiocyanate Anions

Anirban Mondal and Sundaram Balasubramanian*

Chemistry and Physics of Materials Unit, Jawaharlal Nehru Centre for Advanced Scientific Research, Bangalore 560 064, India

Supporting Information

ABSTRACT: A refined set of potential parameters for 1-alkyl-3-methylimidazolium based room temperature ionic liquids with anions such as acetate, dicyanamide, and thiocyanate has been obtained. Site charges of ions were derived through the density-derived electrostatic and charge partitioning (DDEC/c3) method utilizing periodic density functional theory calculations of these liquids. Intermolecular structure and dynamics, in particular, the collective quantities predicted by the refined force field, match experimental results quantitatively.

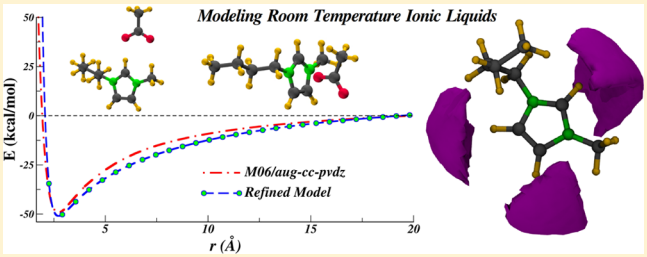

1. INTRODUCTION

Room temperature ionic liquids (RTILs) have attracted significant attention in applied chemistry as novel solvents for synthetic applications, lubricants, in energy applications, actuators, sensors, reaction media, and many more.[1−13] Classical molecular dynamics (MD) simulations based on empirical force fields are apt to study the thermodynamics, structure, and dynamics of such liquids. The need for reliable force fields which represent molecular interactions in an effective and computationally efficient manner is of paramount importance. Although an extensive set of force field parameters for ionic liquids has been developed over the years,[14−35] transferability and the ability to reproduce dynamical properties accurately over a wide range of thermodynamic state points are issues.[31,36−39]

An important aspect of force field for ILs is the transferability of site parameters across ILs. Charge transfer between ions[40] as well as polarization (in particular, that of the anion) in ionic liquids need to be accounted for in an effective manner. Both photoelectron spectroscopy experiments[41−43] as well as quantum density functional theory based simulations[44−49] have demonstrated the nature and magnitude of charge transfer in the condensed state. In order to capture these effects, we have recently outlined a protocol that combines electron density data of an ionic liquid in its condensed phase with gas phase quantum chemical calculations, to yield suitable interaction parameters within a nonpolarizable force field.[49]

In our approach, a charge partitioning method (DDEC/c3) developed by Manz and Sholl[50,51] was employed to obtain the ion charges from crystalline as well as bulk liquid phases of these salts. It was shown that the ions in condensed phases possess fractional charges (between 0.6e and 0.8e). The fractional charges were adapted into the well-established CLaP[14−16] force field. Subsequently, the nonbonded and torsional parameters were refined so as to make them be in accord with the partial charges. This approach showed substantial improvement in predicting the physical properties of seven RTILs, containing different anions.[49,52] The good agreement with experimental data on a wide range of properties gives us confidence in expanding these calculations to other anions commonly used in ILs.

In the present work, refined force field parameters are determined for the IL anions, acetate ([CH_3COO] or [OAc]), thiocyanate ([SCN]), and dicyanamide ([$N(CN)_2$] or [DCA]), which can be combined with imidazolium cation to form the respective ILs. The methodology of parametrization is the same as described earlier.[49] It consists of (i) derivation of atomic partial charges from condensed phase quantum calculations, (ii) reparametrization of nonbonded and torsional potentials via gas phase quantum calculations, and (iii) molecular dynamics simulations of bulk ionic liquids to validate the force field against experimentally determined observables.

This introduction is followed by details of the methodology. The next section discusses the results which is followed by conclusions.

2. METHODOLOGY AND SIMULATION DETAILS

The cation and anion of ionic liquids used in this work are shown in Figure 1. For the cation, the initial set of parameters was taken from the CLaP force field.[14,15] The nomenclature used to describe sites on the imidazolium ring and on the anions is shown in Figure S1 of the Supporting Information. To

Special Issue: Biman Bagchi Festschrift

Received: March 9, 2015
Revised: April 16, 2015
Published: April 23, 2015

DOI: 10.1021/acs.jpcb.5b02272
J. Phys. Chem. B 2015, 119, 11041−11051

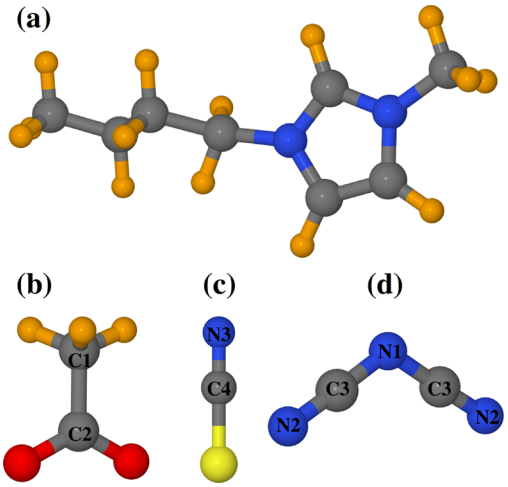

Figure 1. Molecular structure of ions (a) [BMIM], (b) [CH_3COO], (c) [SCN], and (d) [$N(CN)_2$] used in simulations. Color scheme: nitrogen, blue; carbon, gray; hydrogen, orange; oxygen, red; sulfur, yellow.

provide the initial framework for refinement, force fields of Lopes et al.,[17] Senapati et al.,[53] and Chaumont and Wipff[54] for the anions [$N(CN)_2$], [CH_3COO], and [SCN], respectively, were employed.

Charge Derivation from Bulk IL. Our earlier calculations were primarily based on deriving charges from DFT calculations of crystalline phases.[49] It was also shown that the ion charges derived thus matched the mean values of the ion charge distributions obtained through DFT calculations of the corresponding liquid phase. Thus, if the crystal structure of an IL compound is not available, the electron density distribution of its liquid phase can be obtained from a DFT calculation from which the atomic site charges can be obtained. It is this approach that comes in handy for the ILs studied here, for which 1-butyl-3-methylimidazolium is chosen as the common cation.

Classical MD simulations of these liquid systems were carried out with typically around 30 ion pairs using force fields based on the literature as mentioned earlier. A full description of these systems is provided in Table S1 of the Supporting Information. The liquid configurations acquired from MD trajectories were then quenched to their minimum energy positions within the DFT framework using CP2K software.[55] The convergence criteria used for the gradient of electronic wave functions and force on the nuclei were 10^{-7} and 10^{-3}, respectively. The Perdew, Burke, and Ernzerhof (PBE) exchange-correlation functional was employed.[56] The effects of core electrons and nuclei were treated with Geodecker–Teter–Hutter (GTH) pseudopotentials.[57] Triple-ζ double-polarized basis sets with an energy cutoff of 280 Ry were used to represent all the valence electrons. The optimized coordinates were used to generate the valence electron density at the same level of theory and were saved in a cube file. This density information was used as an input to the DDEC/c3 code[50,51] to obtain the atomic charges. The charges were averaged over all ions present in all the configurations quenched similarly from a liquid phase classical MD trajectory.

Short-Range and Torsional Interactions. Another important aspect of modeling ionic liquids is to represent the nonbonded interaction parameters accurately. Those for the imidazolium cation have already been described earlier.[49] Thus, such parameters were refined only for those atoms belonging to the anions studied here. The quantum chemical potential energy surfaces (PES) for ion pairs in the gas phase across three different directions (as shown in Figure S2 of the Supporting Information) have been used as benchmarks. The Lennard-Jones parameters of anions were then iteratively adjusted to reproduce these three different quantum PES. The refined Lennard-Jones parameters for anions are tabulated in Table 1.

Table 1. Lennard-Jones Parameters for Anions According to the Refined Model[a]

atom	ε (kcal mol^{-1})	σ (Å)
C1	0.10939	3.15
C2	0.07599	3.00
O	0.10999	2.56
H	0.01270	2.45
N1	0.16500	3.05
C3	0.06500	3.10
N2	0.16500	3.00
S	0.22000	3.34
C4	0.18000	3.25
N3	0.20000	2.78

[a]Atoms separated by three covalent bonds interact via 1–4 interactions with the following scale factors: 0.5 for Lennard-Jones and 0 for Coulomb.

As changes in nonbonded parameters affect 1–4 interactions as well, the torsional parameters too need to be reworked. These torsional parameters for anions are tabulated in Table 2.

Molecular Dynamics Simulations. 1-Butyl-3-methylimidazolium based ionic liquids containing any of the three anions ([$N(CN)_2$], [CH_3COO], and [SCN]) were modeled using this refined set of force field parameters. Classical MD simulations were performed on their liquid phases using the LAMMPS package.[58] Long-range interactions were computed using the particle–particle particle mesh Ewald (PPPM) solver with a precision of 10^{-5}. The velocity Verlet algorithm was used to calculate the equations of motion with a time step of 1 fs. All C–H covalent bonds were constrained using the SHAKE algorithm as implemented in LAMMPS.[58] The Nosé–Hoover thermostat[59,60] and barostat were employed to control the temperature and pressure of the system. Cross interactions between different atom types were computed using standard Lorentz–Berthelot rules.

All the systems were simulated using 512 ion pairs. Initial configurations were generated using Packmol software.[61] The simulations have been carried out at the same temperatures where experimental data were available in the literature. These were 300, 313, 333, and 343 K for [BMIM][CH_3COO] and [BMIM][$N(CN)_2$], while for the [BMIM][SCN] system, the temperatures were 300, 313, 323, and 333 K. All the systems were equilibrated for 10 ns in the constant-NPT ensemble followed by a duration of 5 ns in the constant-NVT ensemble. This procedure was followed by a 48 ns production run in the constant-NVT ensemble. The systems were visualized in VMD.[62]

The liquid–vapor interface of these ionic liquids was simulated in order to calculate surface tension. To create one, a pre-equilibrated simulation cell containing 512 ion pairs was taken and the cell length along the z-axis was stretched to 100 Å. The pressure tensor at every time step was stored from three independent MD trajectories, each of length 10 ns. The

DOI: 10.1021/acs.jpcb.5b02272
J. Phys. Chem. B 2015, 119, 11041–11051

Table 2. Proper Dihedral Parameters in Multi/Harmonic Form According to the Refined Model: $E^{MH}_{dihedral} = \sum_{n=1}^{5} A_n \cos^{n-1}(\phi)$

	A (kcal mol^{-1})				
dihedrals	A_1	A_2	A_3	A_4	A_5
O−C2−C1−H	0.12146	0.11818	−0.00109	0.08951	0.01109
N2−C3−N1−C3	0.00000	0.00000	0.00000	0.00000	0.00000

diagonal components of the stress tensor were used to calculate surface tension γ defined as

$$\gamma = \frac{l_z}{4}(2P_{zz} - P_{xx} - P_{yy}) \quad (1)$$

where l_z is the length of the simulation box along the z-axis.

The equilibrium Green−Kubo relation was employed to obtain the shear viscosity of these systems using the full stress (pressure) tensor[63]

$$\eta(t) = \frac{V}{10k_BT}\int_0^t \langle Tr[\tilde{\mathbf{P}}(t'')\tilde{\mathbf{P}}(t' + t'')]\rangle \, dt' \quad (2)$$

where V is the system volume and $\tilde{\mathbf{P}}$ is the symmetric, traceless part of the pressure tensor. Twelve independent MD trajectories each of 8 ns duration were generated, and the pressure tensor was stored at every time step. The block average of these trajectories was used to compute the stress autocorrelation function whose time integral (evaluated numerically using the trapezoidal rule) yields the shear viscosity.

In a similar approach, the time integral of the electric current autocorrelation function was used to calculate the electrical conductivity defined as[64,65]

$$\sigma = \frac{1}{3k_BTV}\int_0^\infty \langle \mathbf{j}(t)\cdot\mathbf{j}(0)\rangle \, dt \quad (3)$$

where $\mathbf{j}(t)$ represents the electric-current function

$$\mathbf{j}(t) = \sum_{i=1}^{N} q_i \mathbf{v}_i(t) \quad (4)$$

and q_i and $\mathbf{v}_i(t)$ are the charge and velocity of the ith atom at time t. N is the number of atoms present in the system. A block of 2 ns in length was generated from 20 independent MD trajectories, and atom velocities were stored at every time step. Each trajectory was used to calculate the electric current autocorrelation function, and eq 3 was used to calculate σ.

3. RESULTS AND DISCUSSION

Atomic Charges. The effects of electronic polarization and charge transfer between ions are reflected in the calculated ion charges. The net ion charge showed a reduction from unity in all three liquids. The mean ion charges were ±0.74e, ± 0.65e, and ±0.78e for ionic liquids composed of [CH_3COO], [SCN], and [$N(CN)_2$] anions, respectively. The smaller anion, SCN, exhibits a larger charge transfer effect, nearly similar to the charge of the chloride determined in [BMIM][Cl] liquid earlier.[49] A few important observations: (i) site charges on atoms in the butyl tail as well as in the methyl group attached to the imidazolium cation were similar in nature through different ionic liquids, (ii) the methylene groups present beyond C_2 carbon were found to be charge neutral, (iii) symmetry related atoms in both anions and cations possessed similar charge values. For the sake of transferability, as before,[49] minor reassignments were made in the atomic site charges. For a particular type of anion, site charges of different atom types were averaged over the number of anions present in each system. The residual charge on the terminal methyl group and methylene groups beyond the C_2 carbon were redistributed to other sites on the imidazolium ring so that these nonpolar groups could be assigned a charge of zero. Revised site charges are provided in Tables 3 and 4.

Table 3. Atomic Site Charges (e) for the Cation According to the Refined Model

atom	[OAc]	[SCN]	[DCA]
N	0.135	0.120	0.140
CR	−0.015	−0.005	−0.005
CW	−0.120	−0.110	−0.120
HA	0.175	0.145	0.185
HB	0.165	0.135	0.170
C1	−0.250	−0.250	−0.250
H1	0.120	0.120	0.120
C2	−0.076	−0.076	−0.076
CE	−0.174	−0.174	−0.174
HC	0.098	0.098	0.098
CS	−0.196	−0.196	−0.196
CT	−0.294	−0.294	−0.294

Table 4. Atomic Site Charges (e) for the Anion According to the Refined Model

atom	charge (e)
C1	−0.54
C2	0.73
O	−0.66
H	0.13
N1	−0.56
C3	0.50
N2	−0.61
S	−0.38
C4	0.26
N3	−0.53

Density. This refined set of potential parameters was used to simulate the liquid phases of these salts at four different temperatures. Simulations were carried out in the constant-temperature constant-pressure (NPT) ensemble, and the mean box length was used to compute the density of these ionic liquids. The temperature dependence of density compares well with experiment (within 2% deviation) and is presented in Table 5.

Heat of Vaporization. The enthalpy of vaporization has been computed as

$$\Delta H_{vap} = E_{ion\text{-}pair} - E_{liq} + RT \quad (5)$$

where $E_{ion\text{-}pair}$ is the total energy of an ion pair in the gas phase, E_{liq} represents the total energy per mole of an ion pair in the liquid, and R is the universal gas constant. The vaporization enthalpy (ΔH_{vap}) was calculated for these ionic liquids using

DOI: 10.1021/acs.jpcb.5b02272
J. Phys. Chem. B 2015, 119, 11041−11051

Table 5. Density of Ionic Liquids (g/cm^3) Obtained from MD Simulation Using the Refined Force Field, Compared against Experiment[66−68] [a]

ionic liquid	T (K)	ρ^{Exp}	ρ^{Sim}	$\Delta\rho$ (%)
[BMIM][OAc]	300	1.058	1.056	−0.18
Exp. ref 66	313	1.049	1.046	−0.28
	333	1.031	1.030	−0.09
	343	1.025	1.023	−0.19
[BMIM][DCA]	300	1.059	1.071	1.13
Exp. ref 67	313	1.049	1.061	1.14
	333	1.037	1.045	0.77
	343	1.031	1.037	0.58
[BMIM][SCN]	300	1.069	1.082	1.21
Exp. ref 68	313	1.060	1.070	0.94
	323	1.049	1.062	1.23
	333	1.043	1.053	0.95

[a]The estimated uncertainty in computed density is around 0.004 g/cm^3. $\Delta\rho = (\rho^{Sim} - \rho^{Exp})/\rho^{Exp}$.

the refined model. The results are summarized in Table 6. Values obtained from simulations show good agreement with

Table 6. Heat of Vaporization (kcal/mol) at 300 K of ILs Obtained from Simulations Compared against Experimental Data at 298 K[a]

ionic liquid	ΔH_{vap}^{Exp}	ΔH_{vap}^{Sim}	$\Delta(\Delta H_{vap})$ (%)
[BMIM][OAc]	26.98[69]	30.01	+11.14
[BMIM][DCA]	37.57[70]	33.71	−10.27
[BMIM][SCN]	35.37[71]	30.12	−14.13

[a]The uncertainty in the computed heat of vaporization is around 0.03 kcal/mol. $\Delta(\Delta H_{vap}) = (\Delta H_{vap}^{Sim} - \Delta H_{vap}^{Exp})/\Delta H_{vap}^{Exp}$.

experiment. The heat of vaporization computed for [BMIM]-[DCA] using the current model is comparable to that estimated from a polarizable model (ΔH_{vap} = 31.5 kcal/mol).[72]

Structure. To understand the intermolecular structure in the liquid, site−site radial distribution functions were analyzed. Figure 2a shows the radial distribution functions (RDFs) between the geometric center of the imidazolium ring and the central atom of the corresponding anion. The RDFs between the anion (the anion atom that has the largest negative partial charge and acts as a hydrogen bond acceptor; O in [OAc], N2 in [DCA], and N3 in [SCN]) and the acidic hydrogen (H_A) on imidazolium cation are displayed in Figure 2b.

The intense first peak of cation−anion $g(r)$ indicates a strong structural correlation between the cation and the anion which is observed even at distances of 20 Å (see Figure S4 of the Supporting Information). As can be seen from Figure 2b, the anion−H_A $g(r)$ have a strong, sharp peak around 2 Å, typical of hydrogen bonding. Within a sphere of 4 Å radius, the acidic proton on the imidazolium cation has an average of 2.2 oxygen atoms of [CH_3COO] and 2.0 and 1.4 nitrogen atoms of [$N(CN)_2$] and [SCN], respectively.

The central nitrogen atom (N1) in [$N(CN)_2$] and the sulfur atom in [SCN] also possess a negative partial charge, as shown in Table 4, and hence, in principle, both of them can form hydrogen bonds with the acidic proton of the imidazolium cation. We calculated the $g(r)$ between these two pairs of atoms as well which are displayed in Figure S3 of the Supporting Information. These $g(r)$ show no sign of strong interaction between the nitrogen atom (N1) in [$N(CN)_2$] or the sulfur

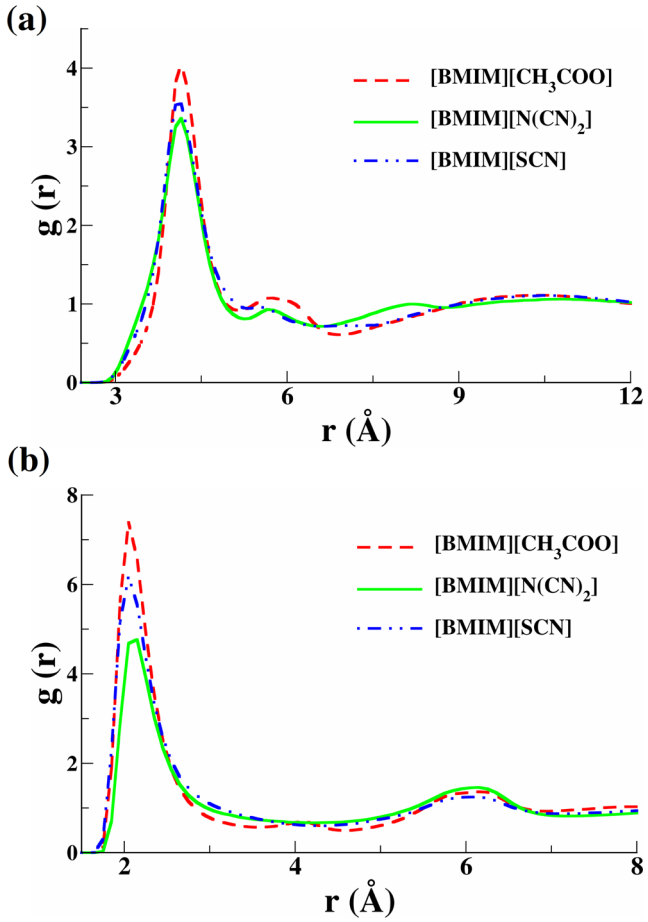

Figure 2. Radial distribution functions for (a) cation−anion and (b) anion−H_A for ionic liquids modeled with refined parameters.

atom in [SCN] with the [BMIM] acidic hydrogen atom, which is consistent with the results obtained earlier.[19,38,73]

The structural correlations were further investigated by examining the spatial density distribution of anion atoms around the cation. Figure 3 displays the spatial density map of the anion around the cation center of mass at an isosurface value of 0.011 Å^{-3}. Three well-defined, preferred locations for anions were seen in all the systems, and they are in the proximity of the three ring hydrogen atoms: one H_A and two H_B atoms. The former, i.e., the acidic hydrogen site (H_A), is more favored.

Surface Tension. Calculated surface tension values are compared against experimental data in Table 7. Computed results showed adequate consistency with experimental observations over the set of state points.

Mean Square Displacement and Self-Diffusion Coefficients. Transport properties are analyzed by calculating the self-diffusion coefficients of ions at different temperatures. The mean square displacements (MSDs) of the center of mass of ions were calculated on the basis of three MD runs each of 30 ns, whose average is presented in Figure 4. At any given time, the lighter anions diffuse faster than cations as expected.[53,74]

The signature of the diffusive nature of molecular motions can be determined from the exponent $\gamma(t)$ defined as

$$\gamma(t) = \frac{d \ln\langle \Delta r^2(t)\rangle}{d \ln(t)} \quad (6)$$

DOI: 10.1021/acs.jpcb.5b02272
J. Phys. Chem. B 2015, 119, 11041−11051

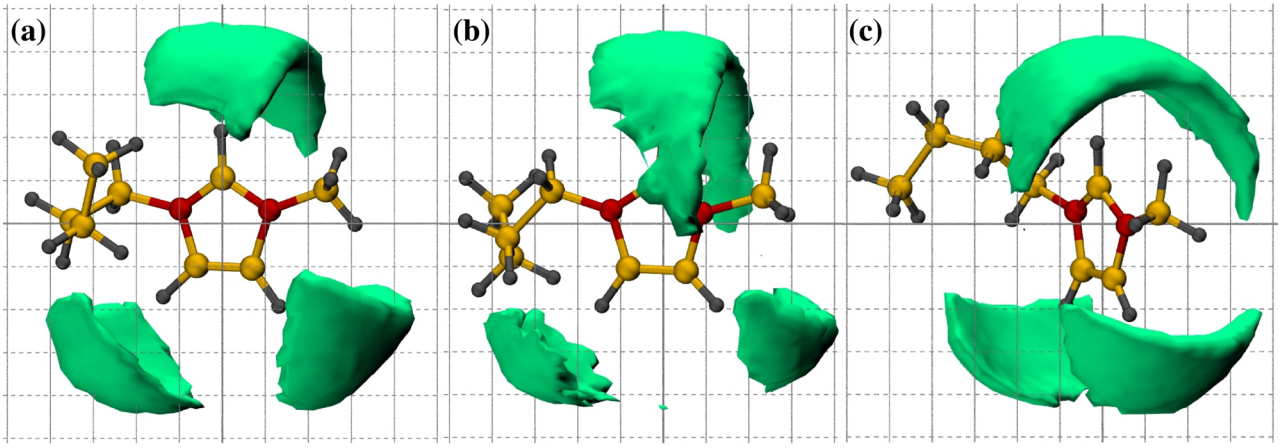

Figure 3. Spatial distribution function of anions around the cation at an isosurface value of 0.011 Å^{-3}: (a) [BMIM][CH_3COO]; (b) [BMIM][$N(CN)_2$]; (c) [BMIM][SCN]. Color scheme: red, nitrogen; orange, carbon; gray, hydrogen.

Table 7. Surface Tension (mN/m) Obtained from MD Simulation Compared against Experiment[66−68] *a*

ionic liquid	T (K)	γ^{Exp}	γ^{Sim}	$\Delta\gamma$ (%)
[BMIM][OAc]	300	36.4	36.7	+0.94
Exp. ref 66	313	35.5	34.2	−3.51
	333	34.7	33.5	−3.52
	343	34.4	32.5	−5.21
[BMIM][DCA]	300	48.6	43.9	−8.21
Exp. ref 67	313	47.2	43.3	−7.81
	333	45.5	41.9	−6.82
	343	45.0	41.2	−8.43
[BMIM][SCN]	300	45.4	41.3	−8.22
Exp. ref 68	313	43.3	39.7	−7.64
	323	39.2	37.3	−4.84
	333		35.9	

*a*The estimated standard error on the mean in the calculated surface tension is around 0.07 mN/m. $\Delta\gamma = (\gamma^{Sim} - \gamma^{Exp})/\gamma^{Exp}$.

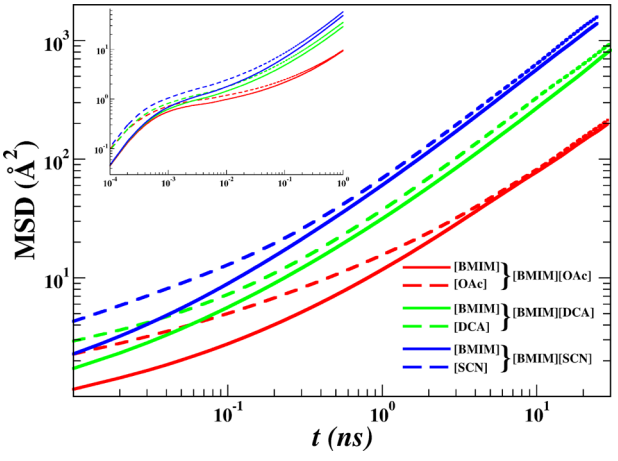

Figure 4. Mean square displacement (MSD) of ions as a function of time at 300 K. The inset shows the MSD at short times focusing on the subdiffusive nature of transport at those time scales.

where $\Delta r^2(t)$ is the mean square displacement at time t. The diffusive regime is characterized by $\gamma(t) = 1$.

We have considered the last 20 ns ($\gamma(t) \simeq 1$, $t \geq 10$ ns; see Figure S5 in the Supporting Information) of the simulation data to acquire ion diffusion coefficients. The computed self-diffusion coefficient of ions at four different temperatures are tabulated in Table S2 of the Supporting Information. The ion self-diffusion coefficients are consistently higher for [BMIM][SCN] compared to [BMIM][OAc] or [BMIM][DCA]. This may be due to the smaller size of the [SCN] anion and the reduced total ion charge (±0.65) in [BMIM][SCN], which results in diminished electrostatic interactions between the ions. A similar trend in ion diffusion coefficients was observed in earlier simulations as well.[53,74]

Viscosity. The initial decay of the stress autocorrelation functions is shown in Figure S6 of the Supporting Information. The equilibrium viscosity was evaluated from the converged value of the running integral of the stress time autocorrelation function using eq 2. Shear viscosity values extracted from MD simulations at different temperatures for the systems investigated here are tabulated in Table 8.

Table 8. Shear Viscosity (mPa·s) of ILs Obtained from MD Simulations, Experimental Values[66−68] *a*

ionic liquid	T (K)	η^{Exp}	η^{Sim}	$\Delta\eta$ (%)
[BMIM][OAc]	300	210.0	191.5 ± 7.0	−8.8
Exp. ref 66	313	112.0	104.3 ± 6.2	−6.8
	333	42.7	38.4 ± 3.2	−10.0
	343	28.7	24.1 ± 3.0	−16.0
[BMIM][DCA]	300	24.4	25.1 ± 3.1	2.8
Exp. ref 67	313	16.8	18.2 ± 2.0	8.3
	333	8.9	8.7 ± 1.8	−2.2
	343	6.6	6.4 ± 1.6	−3.0
[BMIM][SCN]	300	40.9	35.2 ± 4.3	−13.9
Exp. ref 68	313	27.2	24.1 ± 3.3	−11.3
	323	14.1	12.6 ± 2.0	−10.5
	333	10.7	8.1 ± 1.7	−24.2

a$\Delta\eta = (\eta^{Sim} - \eta^{Exp})/\eta^{Exp}$.

The running integral of the stress time correlation function for the ILs [BMIM][OAc] and [BMIM][DCA] is displayed in Figure S7 of the Supporting Information to demonstrate its convergence.

Shear viscosity obtained using this refined potential showed satisfactory agreement with experiments with deviations much less than 20%, as shown in Table 8. The maximum deviation (around 24%) was observed for [BMIM][SCN], for which the computed enthalpy of vaporization was also found to be

DOI: 10.1021/acs.jpcb.5b02272
J. Phys. Chem. B 2015, 119, 11041−11051

underpredicted by maximum margin (14%). This may be due to the underbinding nature of this potential, as the electrostatic interaction is much diminished by the total ion charge (±0.65) as extracted from the DDEC/c3 method. The observed trend in computed viscosities, η[BMIM][OAc] > η[BMIM][SCN] > η[BMIM][DCA], showed good agreement with experiment as well.[66−68] The temperature dependence of viscosities obtained from MD simulations showed acceptable consistency with experiment and is displayed in Figure 5.

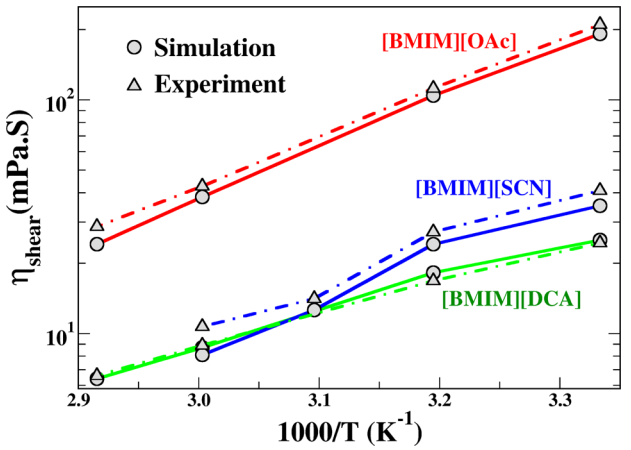

Figure 5. Shear viscosity as a function of temperature obtained from simulations compared against experimental values.[66−68]

Electrical Conductivity. The zero frequency electrical conductivity (σ_{GK}) was estimated from the integral of the electric current time autocorrelation function through the Green−Kubo relation, eq 3. A set of 20 independent trajectories, each of 2 ns in length, was used to compute the electric current autocorrelation functions, and finally, the electrical conductivity was averaged over these trajectories. Electrical conductivity values calculated using eq 3 for these ILs are provided in Table 9.

In correspondence to its low viscosity, [BMIM][DCA] showed the highest electrical conductivity among the three ILs. The order of electrical conductivity from MD simulation, σ[BMIM][DCA] > σ[BMIM][SCN] >σ[BMIM][OAc], agrees with experiment.[75−77] The temperature dependence of electrical conductivities for these ionic liquids is shown in Figure 6. The calculated electrical conductivity values are also

Table 9. Electrical Conductivity (S·m^{-1}) of ILs Evaluated from MD Simulations and Experimental Values[75−77] [a]

ionic liquid	T (K)	σ^{Exp}	σ^{GK}	$\Delta\sigma$ (%)
[BMIM][OAc]	300	0.073	0.070	−4.11
Exp. ref 75	313	0.136	0.129	−5.14
	333	0.359	0.319	−11.14
	343	0.532	0.472	−11.27
[BMIM][DCA]	300	1.052	0.912	−13.30
Exp. ref 76	313	1.570	1.520	−3.18
	333	2.410	2.324	−3.57
	343	2.850	2.716	−4.71
[BMIM][SCN]	300	0.730	0.621	−14.93
Exp. ref 77	313	1.270	1.115	−12.20
	323	1.820	1.514	−16.81
	333	2.260	1.892	−16.28

[a]The uncertainty in computed conductivity is around 0.04 S·m^{-1}. $\Delta\sigma = (\sigma^{Sim} - \sigma^{Exp})/\sigma^{Exp}$.

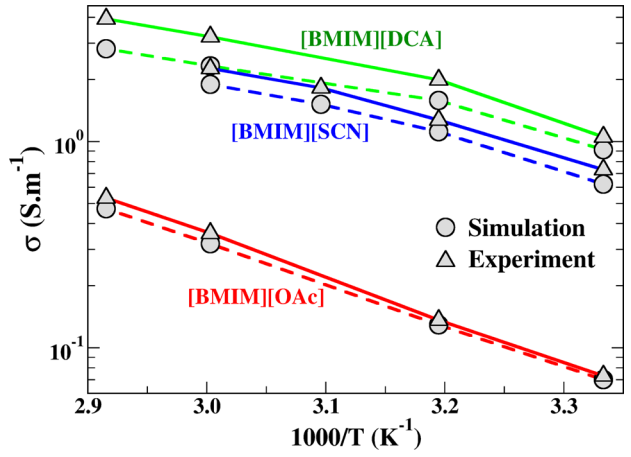

Figure 6. Temperature dependence of electrical conductivity obtained from simulation and plotted against experiment.[75−77]

able to reproduce the experimentally measured conductivities at different temperatures, with the maximum deviation (less than 20%) observed for [BMIM][SCN]. An earlier simulation result obtained for [BMIM][DCA] from a polarizable model[72] underestimated the experiment by only −3% at 298 K, compared to the 13% deviation obtained by us. However, at 333 K, the polarizable model overestimated the conductivity by 24%. The origin of these differences between the models and experiment needs to be investigated further.

Incoherent Intermediate Scattering Function. The self part of the van Hove function,[78] also known as the incoherent (self) intermediate scattering function [$F_s(\mathbf{Q}, t)$], was investigated to discern the nature of relaxation of density correlations of individual ions at different time and length scales (wave vector). This function is defined as[79]

$$F_s(\mathbf{Q}, t) = \frac{1}{N}\sum_i \langle \exp\{-i\mathbf{Q}[\mathbf{r}_i(t) - \mathbf{r}_i(0)]\}\rangle \quad (7)$$

here, N is the number of ions, $\mathbf{r}_i(t)$ is the position of the ion center at time t, and $\mathbf{Q}$ is the reciprocal lattice vector.

$F_s(\mathbf{Q}, t)$ captures the structural relaxation of ILs. At short time scales, $F_s(\mathbf{Q}, t)$ exhibits a fast relaxation (β relaxation) followed by a plateau signifying ions trapped in a cage of counterions. At longer time scales, ions diffuse out, leading to the complete relaxation of $F_s(\mathbf{Q}, t)$ (α relaxation).[80−87] The decay of $F_s(\mathbf{Q}, t)$ for the cation and anion of different ionic liquids at a wave vector value of 1.4 Å^{-1} obtained from simulations is displayed in Figure 7. At all temperatures, the structural relaxation of anions is faster than that of cations in all three ionic liquids, consistent with the trend in self-diffusion.[88]

In order to estimate the time scales associated with $\beta(\tau_\beta)$ and α relaxations (τ_α), $F_s(\mathbf{Q}, t)$ were fitted (see Figure S8 of the Supporting Information) to a modified Kohlrausch−Williams−Watts function[84]

$$F_s(\mathbf{Q}, t) = A\exp(-t/\tau_\beta) + (1 - A)\exp[-(t/\tau_\alpha)^\beta] \quad (8)$$

The mean relaxation time for the α process is given by[84,89]

$$\langle\tau_\alpha\rangle = \frac{\tau_\alpha}{\beta}\Gamma\left(\frac{1}{\beta}\right) \quad (9)$$

DOI: 10.1021/acs.jpcb.5b02272
J. Phys. Chem. B 2015, 119, 11041−11051

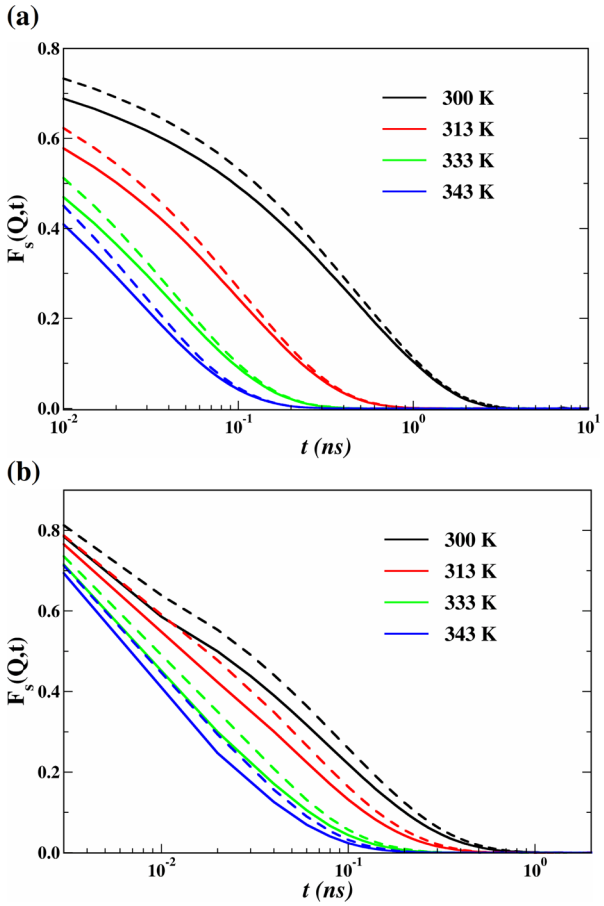

Figure 7. Self-intermediate scattering functions $F_s(\mathbf{Q}, t)$ of cations (dashed line) and anions (solid line) of (a) [BMIM][OAc] and (b) [BMIM][DCA] at different temperatures and at $\mathbf{Q}$ = 1.4 Å^{-1} (the same for [BMIM][SCN] is shown in Figure S9 in the Supporting Information).

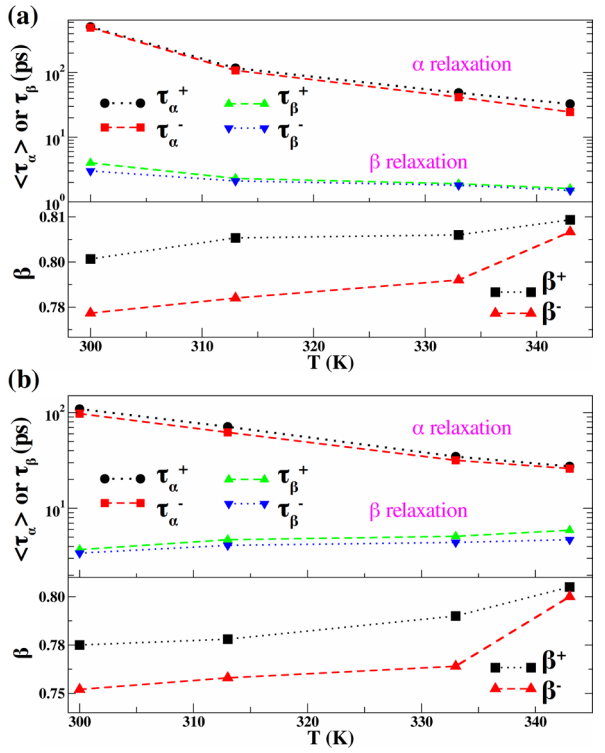

Figure 8. Structural relaxation times τ_β and $\langle\tau_\alpha\rangle$ and the stretching parameter (β) of α relaxation for cations and anions of (a) [BMIM][OAc] and (b) [BMIM][DCA] as a function of temperature.

where Γ is the gamma function. The top panels of Figure 8a and b display the estimated relaxation times $\langle\tau_\alpha\rangle$ and τ_β as a function of temperature in different ILs. A closer investigation showed that τ_α for anions was lower than that for cations, which suggests that the average time to escape from the "cage" formed by their neighboring ions is smaller for anions than that of cations. A similar kind of behavior was also observed in the case of τ_β. The bottom panels of Figure 8a and b display the temperature dependence of the stretching parameters (β) for α relaxation in different ILs. For both cations and anions, β increased with an increase in system temperature. Again, values of β for cations were larger than those of anions. β values for these ILs are larger than those reported for [BMIM][PF_6],[81] presumably due to the lower viscosity of ILs studied here. Further, β^- is marginally smaller than β^+, implying the larger dynamical heterogeneity of anions.

The dependence of $F_s(\mathbf{Q}, t)$ on wave vector is shown in Figure 9. At large $\mathbf{Q}$, the relaxation behaviors for cations and anions in [BMIM][OAc] are quite similar, while in [BMIM]-[DCA] (or in [BMIM][SCN], Figure S9 in the Supporting Information), their relaxations are decoupled. At smaller $\mathbf{Q}$, anions show a faster relaxation than cations. Thus, these observations suggest that the "caging" dynamics is critical in these systems, consistent with earlier results obtained from both experiment and simulation.[90,91]

Coherent Intermediate Scattering Function. In order to investigate the collective behavior of the system, we have computed the coherent intermediate scattering function $F(\mathbf{Q}, t)$ defined as[79]

$$F(\mathbf{Q}, t) = \frac{1}{N}\sum_i \sum_j \langle \exp\{-i\mathbf{Q}[\mathbf{r}_i(t) - \mathbf{r}_j(0)]\}\rangle \quad (10)$$

The relaxation of $F(\mathbf{Q}, t)$ at different wave vectors ($\mathbf{Q}$) at 300 K is displayed in Figure 10. $F(\mathbf{Q}, t)$ showed a two-step relaxation process similar to what was observed in the case of $F_s(\mathbf{Q}, t)$.

4. CONCLUSIONS

We have prescribed a method to obtain atomic site charges employing periodic density functional theory on the liquid phase of ionic liquids. This approach extends our earlier work[49] which used the DDEC/c3 method[50,51] on both the crystalline and liquid phases of ionic liquids to obtain atomic charges. The electronic polarization and charge transfer effects are accounted for in an effective manner. A 1-butyl-3-methylimidazolium based cation combined with three different anion types—acetate (CH_3COO), dicyanamide ($N(CN)_2$), and thiocyanate (SCN)—were considered. As before, charges on ions were less than unity and were calculated to be −0.78e, −0.74e, and −0.65e for DCA, OAc, and SCN, respectively.

In order to obtain a transferable force field, this set of partial charges was combined with the well established CLaP force field developed by Lopes and co-workers.[14−18] Consequently, its nonbonded, 1−4, and torsional interaction parameters were refined. In this refinement procedure, we have adopted three potential energy surface scans in the gas phase for isolated ion pairs as our benchmark. Lennard-Jones parameters which best

DOI: 10.1021/acs.jpcb.5b02272
J. Phys. Chem. B 2015, 119, 11041−11051

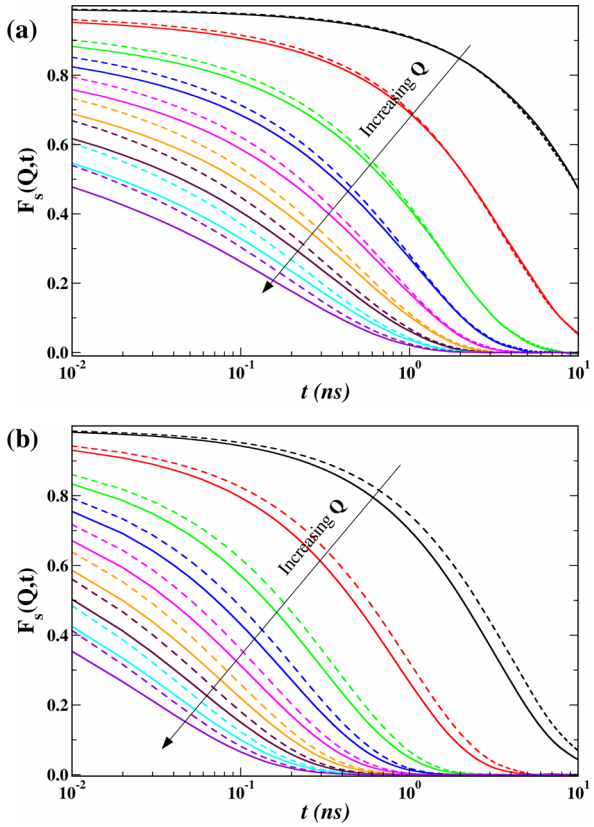

Figure 9. $F_s(\mathbf{Q}, t)$ of cations (dashed lines) and anions (solid lines) of (a) [BMIM][OAc] and (b) [BMIM][DCA] at 300 K and at different wave vectors. Following are the values of **Q** (from top to bottom, in $Å^{-1}$): 0.25, 0.5, 0.8, 1.0, 1.2, 1.4, 1.6, 1.8, and 2.0 (the same for [BMIM][SCN] has been shown in Figure S9 in the Supporting Information).

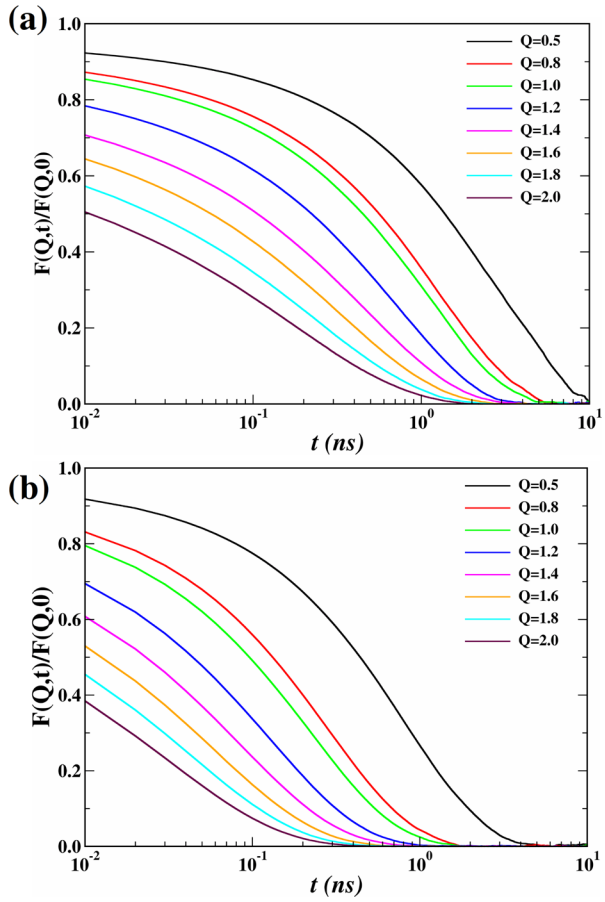

Figure 10. Wave vector dependence of normalized $F(\mathbf{Q}, t)$ at 300 K for (a) [BMIM][OAc] and (b) [BMIM][DCA].

fitted all three of these scans were taken for the condensed phase simulations.

The current scheme considers explicitly the effect of charge transfer between ions, while the effect of polarization in the condensed state is captured in an effective, mean field sense. The exact contribution of each of these effects which resulted in bettering the prediction of transport properties is unknown and could be an object of study in the future. The force field parameters are transferable, and it is possible to study ILs containing imidazolium cations with varying alkyl tail length. The transferability of the parameters across temperature has been demonstrated to the best extent possible—through the nearly quantitative reproduction of density, surface tension, shear viscosity, and electrical conductivity. Thus, we are confident that the parameters are robust.

Classical molecular dynamics simulations have been carried out for the three ionic liquids modeled with this new set of potential parameters at four different state points. Computed static properties, such as density, heat of vaporization, and surface tension, were in good agreement with experimental data. Various methods were employed to compute transport properties including self-diffusion coefficients, ionic conductivity, and shear viscosity. Results from simulations were consistent with the experimental findings. Cations were observed to diffuse slower than anions, consistent with previous simulations.[53,74] Single ion dynamics were investigated through the incoherent intermediate scattering function. The results suggested that the anions possess a marginally higher dynamically heterogeneous environment than the cations.

The Green−Kubo formulation was employed to calculate the ionic conductivity and shear viscosity of the liquids. These collective quantities were predicted to within 20−25% of experimental results, which is not unreasonable given the complexity of these fluids. Despite these differences, this nonpolarizable force field can reproduce the experimental trends with temperature remarkably well. A drawback of the current approach is in modeling mixtures of ILs having the same cation but different anions. In the current framework, the cation charges in the two pure ILs are different, which poses an issue when the ILs are mixed. We hope to address such challenges in the future.

■ ASSOCIATED CONTENT

Supporting Information

Atom labeling in cation and anions, description of liquid systems studied for charge calculation, potential energy surface scan, site−site radial distribution functions, β exponent as a function of time, self-diffusion coefficients, running values of shear viscosities, and self-intermediate scattering functions for cations and anions. The Supporting Information is available free of charge on the ACS Publications website at DOI: 10.1021/acs.jpcb.5b02272.

DOI: 10.1021/acs.jpcb.5b02272
J. Phys. Chem. B 2015, 119, 11041−11051

AUTHOR INFORMATION

Corresponding Author

*Phone: +91 (80) 2208 2808. Fax: +91 (80) 2208 2766. E-mail: bala@jncasr.ac.in.

Notes

The authors declare no competing financial interest.

ACKNOWLEDGMENTS

We thank DST for support. S.B. thanks Sheikh Saqr Laboratory, JNCASR, for a senior fellowship. We thank the Centre for the Development of Advanced Computing, Bangalore, where a part of the computations were carried out.

REFERENCES

(1) Hallett, J. P.; Welton, T. Room-Temperature Ionic Liquids: Solvents for Synthesis and Catalysis. 2. *Chem. Rev.* **2011**, *111*, 3508−3576.

(2) Dupont, J. From Molten Salts to Ionic Liquids: A Nano Journey. *Acc. Chem. Res.* **2011**, *44*, 1223−1231.

(3) Brennecke, J. F.; Gurkan, B. E. Ionic Liquids for CO_2 Capture and Emission Reduction. *J. Phys. Chem. Lett.* **2010**, *1*, 3459−3464.

(4) Gurkan, B.; Goodrich, B. F.; Mindrup, E. M.; Ficke, L. E.; Massel, M.; Seo, S.; Senftle, T. P.; Wu, H.; Glaser, M. F.; Shah, J. K.; et al. Molecular Design of High Capacity, Low Viscosity, Chemically Tunable Ionic Liquids for CO_2 Capture. *J. Phys. Chem. Lett.* **2010**, *1*, 3494−3499.

(5) Wishart, J. F. Energy Applications of Ionic Liquids. *Energy Environ. Sci.* **2009**, *2*, 956−961.

(6) Anderson, J. L.; Dixon, J. K.; Brennecke, J. F. Solubility of CO_2, CH_4, C_2H_6, C_2H_4, O_2, and N_2 in 1-Hexyl-3-methylpyridinium Bis(trifluoromethylsulfonyl)imide: Comparison to Other Ionic Liquids. *Acc. Chem. Res.* **2007**, *40*, 1208−1216.

(7) Jin, C.-M.; Ye, C.; Phillips, B. S.; Zabinski, J. S.; Liu, X.; Liu, W.; Shreeve, J. M. Polyethylene Glycol Functionalized Dicationic Ionic Liquids with Alkyl or Polyfluoroalkyl Substituents as High Temperature Lubricants. *J. Mater. Chem.* **2006**, *16*, 1529−1535.

(8) Shin, J.-H.; Henderson, W. A.; Passerini, S. Ionic Liquids to the Rescue? Overcoming the Ionic Conductivity Limitations of Polymer Electrolytes. *Electrochem. Commun.* **2003**, *5*, 1016−1020.

(9) Liu, Y.; Shi, L.; Wang, M.; Li, Z.; Liu, H.; Li, J. A Novel Room Temperature Ionic Liquid Sol-gel Matrix for Amperometric Biosensor Application. *Green Chem.* **2005**, *7*, 655−658.

(10) Ding, J.; Zhou, D.; Spinks, G.; Wallace, G.; Forsyth, S.; Forsyth, M.; MacFarlane, D. Use of Ionic Liquids as Electrolytes in Electromechanical Actuator Systems Based on Inherently Conducting Polymers. *Chem. Mater.* **2003**, *15*, 2392−2398.

(11) Mondal, J.; Choi, E.; Yethiraj, A. Atomistic Simulations of Poly(ethylene oxide) in Water and an Ionic Liquid at Room Temperature. *Macromolecules* **2014**, *47*, 438−446.

(12) Mondal, T.; Das, A. K.; Sasmal, D. K.; Bhattacharyya, K. Excited State Proton Transfer in Ionic Liquid Mixed Micelles. *J. Phys. Chem. B* **2010**, *114*, 13136−13142.

(13) Lynden-Bell, R. M.; Xue, L.; Tamas, G.; Quitevis, E. L. Local Structure and Intermolecular Dynamics of An Equimolar Benzene and 1,3-Dimethylimidazolium Bis[(trifluoromethane)sulfonyl]amide Mixture: Molecular Dynamics Simulations and OKE Spectroscopic Measurements. *J. Chem. Phys.* **2014**, *141*, 044506.

(14) Canongia Lopes, J. N.; Deschamps, J.; Pádua, A. A. H. Modeling Ionic Liquids Using a Systematic All-Atom Force Field. *J. Phys. Chem. B* **2004**, *108*, 2038−2047.

(15) Canongia Lopes, J. N.; Deschamps, J.; Pádua, A. A. H. Modeling Ionic Liquids Using a Systematic All-Atom Force Field. *J. Phys. Chem. B* **2004**, *108*, 11250−11250.

(16) Canongia Lopes, J. N.; Pádua, A. A. H. Molecular Force Field for Ionic Liquids Composed of Triflate or Bistriflylimide Anions. *J. Phys. Chem. B* **2004**, *108*, 16893−16898.

(17) Canongia Lopes, J. N.; Pádua, A. A. H. Molecular Force Field for Ionic Liquids III: Imidazolium, Pyridinium, and Phosphonium Cations; Chloride, Bromide, and Dicyanamide Anions. *J. Phys. Chem. B* **2006**, *110*, 19586−19592.

(18) Canongia Lopes, J. N.; Pádua, A. A. H.; Shimizu, K. Molecular Force Field for Ionic Liquids IV: Trialkylimidazolium and Alkoxycarbonyl-Imidazolium Cations; Alkylsulfonate and Alkylsulfate Anions. *J. Phys. Chem. B* **2008**, *112*, 5039−5046.

(19) Liu, Z.; Huang, S.; Wang, W. A Refined Force Field for Molecular Simulation of Imidazolium-Based Ionic Liquids. *J. Phys. Chem. B* **2004**, *108*, 12978−12989.

(20) Liu, Z.; Chen, T.; Bell, A.; Smit, B. Improved United-Atom Force Field for 1-Alkyl-3-methylimidazolium Chloride. *J. Phys. Chem. B* **2010**, *114*, 4572−4582.

(21) Liu, Z.; Chen, T.; Bell, A. T.; Smit, B. Improved United-Atom Force Field for 1-Alkyl-3-methylimidazolium Chloride. *J. Phys. Chem. B* **2010**, *114*, 10692−10692.

(22) Zhong, X.; Liu, Z.; Cao, D. Improved Classical United-Atom Force Field for Imidazolium-Based Ionic Liquids: Tetrafluoroborate, Hexafluorophosphate, Methylsulfate, Trifluoromethylsulfonate, Acetate, Trifluoroacetate, and Bis(trifluoromethylsulfonyl)amide. *J. Phys. Chem. B* **2011**, *115*, 10027−10040.

(23) Sambasivarao, S. V.; Acevedo, O. Development of OPLS-AA Force Field Parameters for 68 Unique Ionic Liquids. *J. Chem. Theory Comput.* **2009**, *5*, 1038−1050.

(24) Wang, Y.; Izvekov, S.; Yan, T.; Voth, G. A. Multiscale Coarse-Graining of Ionic Liquids. *J. Phys. Chem. B* **2006**, *110*, 3564−3575.

(25) Wang, Y.; Jiang, W.; Yan, T.; Voth, G. A. Understanding Ionic Liquids through Atomistic and Coarse-Grained Molecular Dynamics Simulations. *Acc. Chem. Res.* **2007**, *40*, 1193−1199.

(26) Yan, T.; Burnham, C. J.; Del Pópolo, M. G.; Voth, G. A. Molecular Dynamics Simulation of Ionic Liquids: The Effect of Electronic Polarizability. *J. Phys. Chem. B* **2004**, *108*, 11877−11881.

(27) Yan, T.; Li, S.; Jiang, W.; Gao, X.; Xiang, B.; Voth, G. A. Structure of the Liquid-Vacuum Interface of Room-Temperature Ionic Liquids: A Molecular Dynamics Study. *J. Phys. Chem. B* **2006**, *110*, 1800−1806.

(28) Jiang, W.; Yan, T.; Wang, Y.; Voth, G. A. Molecular Dynamics Simulation of the Energetic Room-Temperature Ionic Liquid, 1-Hydroxyethyl-4-amino-1,2,4-triazolium Nitrate (HEATN). *J. Phys. Chem. B* **2008**, *112*, 3121−3131.

(29) Bhargava, B. L.; Balasubramanian, S.; Klein, M. L. Modelling Room Temperature Ionic Liquids. *Chem. Commun.* **2008**, 3339−3351.

(30) Köddermann, T.; Paschek, D.; Ludwig, R. Ionic Liquids: Dissecting the Enthalpies of Vaporization. *ChemPhysChem* **2008**, *9*, 549−555.

(31) Köddermann, T.; Paschek, D.; Ludwig, R. Molecular Dynamic Simulations of Ionic Liquids: A Reliable Description of Structure, Thermodynamics and Dynamics. *ChemPhysChem* **2007**, *8*, 2464−2470.

(32) Maginn, E. J. Atomistic Simulation of the Thermodynamic and Transport Properties of Ionic Liquids. *Acc. Chem. Res.* **2007**, *40*, 1200−1207.

(33) Choi, E.; McDaniel, J. G.; Schmidt, J. R.; Yethiraj, A. First-Principles, Physically Motivated Force Field for the Ionic Liquid [BMIM][BF_4]. *J. Phys. Chem. Lett.* **2014**, *5*, 2670−2674.

(34) Roy, D.; Maroncelli, M. An Improved Four-Site Ionic Liquid Model. *J. Phys. Chem. B* **2010**, *114*, 12629−12631.

(35) Maginn, E. J. Molecular Simulation of Ionic Liquids: Current Status and Future Opportunities. *J. Phys.: Condens. Matter* **2009**, *21*, 373101.

(36) Qiao, B.; Krekeler, C.; Berger, R.; Delle Site, L.; Holm, C. Effect of Anions on Static Orientational Correlations, Hydrogen Bonds, and Dynamics in Ionic Liquids: A Simulational Study. *J. Phys. Chem. B* **2008**, *112*, 1743−1751.

(37) Dommert, F.; Schmidt, J.; Qiao, B.; Zhao, Y.; Krekeler, C.; Delle Site, L.; Berger, R.; Holm, C. A Comparative Study of Two Classical Force Fields on Statics and Dynamics of [EMIM][BF_4] Investigated

DOI: 10.1021/acs.jpcb.5b02272
J. Phys. Chem. B 2015, 119, 11041−11051

via Molecular Dynamics Simulations. *J. Chem. Phys.* **2008**, *129*, 224501.
(38) Bhargava, B. L.; Balasubramanian, S. Refined Potential Model for Atomistic Simulations of Ionic Liquid [bmim][PF_6]. *J. Chem. Phys.* **2007**, *127*, 114510.
(39) Cadena, C.; Zhao, Q.; Snurr, R. Q.; Maginn, E. J. Molecular Modeling and Experimental Studies of the Thermodynamic and Transport Properties of Pyridinium-Based Ionic Liquids. *J. Phys. Chem. B* **2006**, *110*, 2821−2832.
(40) Dommert, F.; Wendler, K.; Berger, R.; Delle Site, L.; Holm, C. Force Fields for Studying the Structure and Dynamics of Ionic Liquids: A Critical Review of Recent Developments. *ChemPhysChem* **2012**, *13*, 1625−1637.
(41) Blundell, R. K. Licence, P. Tuning Cation-anion Interactions in Ionic Liquids by Changing the Conformational Flexibility of the Cation. *Chem. Commun.* **2014**, *50*, 12080−12083.
(42) Hurisso, B. B.; Lovelock, K. R. J.; Licence, P. Amino Acid-based Ionic Liquids: Using XPS to Probe the Electronic Environment via Binding Energies. *Phys. Chem. Chem. Phys.* **2011**, *13*, 17737−17748.
(43) Men, S.; Lovelock, K. R. J.; Licence, P. X-ray Photoelectron Spectroscopy of Pyrrolidinium-based Ionic Liquids: Cation-anion Interactions and a Comparison to Imidazolium-based Analogues. *Phys. Chem. Chem. Phys.* **2011**, *13*, 15244−15255.
(44) Chaban, V. Polarizability Versus Mobility: Atomistic Force Field for Ionic Liquids. *Phys. Chem. Chem. Phys.* **2011**, *13*, 16055−16062.
(45) Morrow, T. I.; Maginn, E. J. Molecular Dynamics Study of the Ionic Liquid 1-n-Butyl-3-methylimidazolium Hexafluorophosphate. *J. Phys. Chem. B* **2002**, *106*, 12807−12813.
(46) Schröder, C. Comparing Reduced Partial Charge Models with Polarizable Simulations of Ionic Liquids. *Phys. Chem. Chem. Phys.* **2012**, *14*, 3089−3102.
(47) Dommert, F.; Wendler, K.; Qiao, B.; Site, L. D.; Holm, C. Generic Force Fields for Ionic Liquids. *J. Mol. Liq.* **2014**, *192*, 32−37.
(48) Zhang, Y.; Maginn, E. J. A Simple AIMD Approach to Derive Atomic Charges for Condensed Phase Simulation of Ionic Liquids. *J. Phys. Chem. B* **2012**, *116*, 10036−10048.
(49) Mondal, A.; Balasubramanian, S. Quantitative Prediction of Physical Properties of Imidazolium Based Room Temperature Ionic Liquids through Determination of Condensed Phase Site Charges: A Refined Force Field. *J. Phys. Chem. B* **2014**, *118*, 3409−3422.
(50) Manz, T. A.; Sholl, D. S. Chemically Meaningful Atomic Charges That Reproduce the Electrostatic Potential in Periodic and Nonperiodic Materials. *J. Chem. Theory Comput.* **2010**, *6*, 2455−2468.
(51) Manz, T. A.; Sholl, D. S. Improved Atoms-in-Molecule Charge Partitioning Functional for Simultaneously Reproducing the Electrostatic Potential and Chemical States in Periodic and Nonperiodic Materials. *J. Chem. Theory Comput.* **2012**, *8*, 2844−2867.
(52) Mondal, A.; Balasubramanian, S. A Molecular Dynamics Study of Collective Transport Properties of Imidazolium-Based Room-Temperature Ionic Liquids. *J. Chem. Eng. Data* **2014**, *59*, 3061−3068.
(53) Chandran, A.; Prakash, K.; Senapati, S. Structure and Dynamics of Acetate Anion-based Ionic Liquids from Molecular Dynamics Study. *Chem. Phys.* **2010**, *374*, 46−54.
(54) Chaumont, A.; Wipff, G. Solvation of Ln(III) Lanthanide Cations in the [BMI][SCN], [$MeBu_3N$][SCN], and [BMI]$_5$[Ln(NCS)$_8$] Ionic Liquids: A Molecular Dynamics Study. *Inorg. Chem.* **2009**, *48*, 4277−4289.
(55) Hutter, J.; Iannuzzi, M.; Schiffmann, F.; VandeVondele, J. CP2K: Atomistic Simulations of Condensed Matter Systems. *Wiley Interdiscip. Rev.: Comput. Mol. Sci.* **2014**, *4*, 15−25.
(56) Perdew, J. P.; Burke, K.; Ernzerhof, M. Generalized Gradient Approximation Made Simple. *Phys. Rev. Lett.* **1996**, *77*, 3865−3868.
(57) Goedecker, S.; Teter, M.; Hutter, J. Separable Dual-space Gaussian Pseudopotentials. *Phys. Rev. B* **1996**, *54*, 1703−1710.
(58) Plimpton, S. Fast Parallel Algorithms for Short-Range Molecular Dynamics. *J. Comput. Phys.* **1995**, *117*, 1−19.
(59) Nosé, S. A. Unified Formulation of the Constant Temperature Molecular Dynamics Methods. *J. Chem. Phys.* **1984**, *81*, 511−519.
(60) Hoover, W. G. Canonical Dynamics: Equilibrium Phase-space Distributions. *Phys. Rev. A* **1985**, *31*, 1695−1697.
(61) Martínez, L.; Andrade, R.; Birgin, E. G.; Martínez, J. M. PACKMOL: A Package for Building Initial Configurations for Molecular Dynamics Simulations. *J. Comput. Chem.* **2009**, *30*, 2157−2164.
(62) Humphrey, W.; Dalke, A.; Schulten, K. VMD: Visual Molecular Dynamics. *J. Mol. Graphics* **1996**, *14*, 33−38.
(63) Daivis, P. J.; Evans, D. J. Comparison of Constant Pressure and Constant Volume Nonequilibrium Simulations of Sheared Model Decane. *J. Chem. Phys.* **1994**, *100*, 541−547.
(64) Harada, M.; Yamanaka, A.; Tanigaki, M.; Tada, Y. Mass and Size Effects on the Transport Properties of Molten Salts. *J. Chem. Phys.* **1982**, *76*, 1550−1556.
(65) Hansen, J.-P.; McDonald, I. R. *Theory of Simple Liquids*, 3rd ed.; Academic Press: 2006.
(66) Almeida, H. F. D.; Passos, H.; Lopes-da Silva, J. A.; Fernandes, A. M.; Freire, M. G.; Coutinho, J. A. P. Thermophysical Properties of Five Acetate-Based Ionic Liquids. *J. Chem. Eng. Data* **2012**, *57*, 3005−3013.
(67) Sánchez, L. G.; Espel, J. R.; Onink, F.; Meindersma, G. W.; Haan, A. B. Density, Viscosity, and Surface Tension of Synthesis Grade Imidazolium, Pyridinium, and Pyrrolidinium Based Room Temperature Ionic Liquids. *J. Chem. Eng. Data* **2009**, *54*, 2803−2812.
(68) Vakili-Nezhaad, G.; Vatani, M.; Asghari, M.; Ashour, I. Effect of Temperature on the Physical Properties of 1-Butyl-3-methylimidazolium Based Ionic Liquids with Thiocyanate and Tetrafluoroborate Anions, and 1-Hexyl-3-methylimidazolium with Tetrafluoroborate and Hexafluorophosphate Anions. *J. Chem. Thermodyn.* **2012**, *54*, 148−154.
(69) Ma, X.-X.; Wei, J.; Zhang, Q.-B.; Tian, F.; Feng, Y.-Y.; Guan, W. Prediction of Thermophysical Properties of Acetate-Based Ionic Liquids Using Semiempirical Methods. *Ind. Eng. Chem. Res.* **2013**, *52*, 9490−9496.
(70) Chambreau, S. D.; Vaghjiani, G. L.; To, A.; Koh, C.; Strasser, D.; Kostko, O.; Leone, S. R. Heats of Vaporization of Room Temperature Ionic Liquids by Tunable Vacuum Ultraviolet Photoionization. *J. Phys. Chem. B* **2010**, *114*, 1361−1367.
(71) Deyko, A.; Lovelock, K. R. J.; Corfield, J.-A.; Taylor, A. W.; Gooden, P. N.; Villar-Garcia, I. J.; Licence, P.; Jones, R. G.; Krasovskiy, V. G.; Chernikova, E. A.; et al. Measuring and Predicting $\Delta_{vap}H_{298}$ Values of Ionic Liquids. *Phys. Chem. Chem. Phys.* **2009**, *11*, 8544−8555.
(72) Borodin, O. Polarizable Force Field Development and Molecular Dynamics Simulations of Ionic Liquids. *J. Phys. Chem. B* **2009**, *113*, 11463−11478.
(73) Payal, R. S.; Balasubramanian, S. Homogenous Mixing of Ionic Liquids: Molecular Dynamics Simulations. *Phys. Chem. Chem. Phys.* **2013**, *15*, 21077−21083.
(74) Bedrov, D.; Borodin, O. Thermodynamic, Dynamic, and Structural Properties of Ionic Liquids Comprised of 1-Butyl-3-methylimidazolium Cation and Nitrate, Azide, or Dicyanamide Anions. *J. Phys. Chem. B* **2010**, *114*, 12802−12810.
(75) Xu, A.; Zhang, Y.; Li, Z.; Wang, J. Viscosities and Conductivities of 1-Butyl-3-methylimidazolium Carboxylates Ionic Liquids at Different Temperatures. *J. Chem. Eng. Data* **2012**, *57*, 3102−3108.
(76) Yoshida, Y.; Baba, O.; Saito, G. Ionic Liquids Based on Dicyanamide Anion: Influence of Structural Variations in Cationic Structures on Ionic Conductivity. *J. Phys. Chem. B* **2007**, *111*, 4742−4749.
(77) Sterner, E. S.; Rosol, Z. P.; Gross, E. M.; Gross, S. M. Thermal Analysis and Ionic Conductivity of Ionic Liquid Containing Composites with Different Crosslinkers. *J. Appl. Polym. Sci.* **2009**, *114*, 2963−2970.
(78) van Hove, L. Correlations in Space and Time and Born Approximation Scattering in Systems of Interacting Particles. *Phys. Rev.* **1954**, *95*, 249−262.
(79) Herwig, K. W.; Wu, Z.; Dai, P.; Taub, H.; Hansen, F. Y. Quasielastic Neutron Scattering and Molecular Dynamics Simulation

DOI: 10.1021/acs.jpcb.5b02272
J. Phys. Chem. B 2015, 119, 11041−11051

Studies of the Melting Transition in Butane and Hexane Monolayers Adsorbed on Graphite. *J. Chem. Phys.* **1997**, *107*, 5186−5196.
(80) Del Pópolo, M. G.; Voth, G. A. On the Structure and Dynamics of Ionic Liquids. *J. Phys. Chem. B* **2004**, *108*, 1744−1752.
(81) Sarangi, S. S.; Zhao, W.; Müller-Plathe, F.; Balasubramanian, S. Correlation between Dynamic Heterogeneity and Local Structure in a Room-Temperature Ionic Liquid: A Molecular Dynamics Study of [bmim][PF_6]. *ChemPhysChem* **2010**, *11*, 2001−2010.
(82) Habasaki, J.; Ngai, K. L. Heterogeneous Dynamics of Ionic Liquids from Molecular Dynamics Simulations. *J. Chem. Phys.* **2008**, *129*, 194501.
(83) Liu, H.; Maginn, E. A Molecular Dynamics Investigation of the Structural and Dynamic Properties of the Ionic Liquid 1- n-Butyl-3-methylimidazolium Bis(trifluoromethanesulfonyl)imide. *J. Chem. Phys.* **2011**, *135*, 124507.
(84) Triolo, A.; Russina, O.; Arrighi, V.; Juranyi, F.; Janssen, S.; Gordon, C. M. Quasielastic Neutron Scattering Characterization of the Relaxation Processes in a Room Temperature Ionic Liquid. *J. Chem. Phys.* **2003**, *119*, 8549−8557.
(85) Ishida, T.; Shirota, H. Dicationic versus Monocationic Ionic Liquids: Distinctive Ionic Dynamics and Dynamical Heterogeneity. *J. Phys. Chem. B* **2013**, *117*, 1136−1150.
(86) Hu, Z.; Margulis, C. J. Heterogeneity in a Room-temperature Ionic Liquid: Persistent Local Environments and the Red-edge Effect. *Proc. Natl. Acad. Sci. U.S.A.* **2006**, *103*, 831−836.
(87) Pal, T.; Biswas, R. Slow Solvation in Ionic Liquids: Connections to Non-Gaussian Moves and Multi-point Correlations. *J. Chem. Phys.* **2014**, *141*, 104501.
(88) Zhang, Y.; Maginn, E. J. Direct Correlation between Ionic Liquid Transport Properties and Ion Pair Lifetimes: A Molecular Dynamics Study. *J. Phys. Chem. Lett.* **2015**, *6*, 700−705.
(89) Müller-Plathe, F.; van Gunsteren, W. F. Computer Simulation of a Polymer Electrolyte: Lithium Iodide in Amorphous Poly(ethylene oxide). *J. Chem. Phys.* **1995**, *103*, 4745−4756.
(90) Shirota, H.; Castner, E. W. Physical Properties and Intermolecular Dynamics of an Ionic Liquid Compared with Its Isoelectronic Neutral Binary Solution. *J. Phys. Chem. A* **2005**, *109*, 9388−9392.
(91) Hu, Z.; Huang, X.; Annapureddy, H. V. R.; Margulis, C. J. Molecular Dynamics Study of the Temperature-Dependent Optical Kerr Effect Spectra and Intermolecular Dynamics of Room Temperature Ionic Liquid 1-Methoxyethylpyridinium Dicyanoamide. *J. Phys. Chem. B* **2008**, *112*, 7837−7849.

DOI: 10.1021/acs.jpcb.5b02272
J. Phys. Chem. B 2015, 119, 11041−11051